

OPEN

Mobile continuous-flow isotope-ratio mass spectrometer system for automated measurements of N₂ and N₂O fluxes in fertilized cropping systems

Daniel I. Warner¹, Clemens Scheer^{1,2}, Johannes Friedl¹, David W. Rowlings¹, Christian Brunk¹ & Peter R. Grace¹

The use of synthetic N fertilizers has grown exponentially over the last century, with severe environmental consequences. Most of the reactive N will ultimately be removed by denitrification, but estimates of denitrification are highly uncertain due to methodical constraints of existing methods. Here we present a novel, mobile isotope ratio mass spectrometer system (Field-IRMS) for *in-situ* quantification of N₂ and N₂O fluxes from fertilized cropping systems. The system was tested in a sugarcane field continuously monitoring N₂ and N₂O fluxes for 7 days following fertilization using a fully automated measuring cycle. The detection limit of the Field-IRMS proved to be highly sensitive for N₂ (54 g ha⁻¹ day⁻¹) and N₂O (0.25 g ha⁻¹ day⁻¹) emissions. The main product of denitrification was N₂ with total denitrification losses of up to 1.3 kg N ha⁻¹ day⁻¹. These losses demonstrate sugarcane systems in Australia are a hotspot for denitrification where high emissions of N₂O and N₂ can be expected. The new Field-IRMS allows for the direct and highly sensitive detection of N₂ and N₂O fluxes in real time at a high temporal resolution, which will help to improve our quantitative understanding of denitrification in fertilized cropping systems.

In the last 50 years, the use of synthetic nitrogen (N) fertilizers, cultivation of leguminous crops, and fossil fuel combustion have more than doubled the input of reactive nitrogen (N_r – all nitrogen species other than dinitrogen N₂) into the environment. As a result, the global N cycle is even more severely altered by human activity than the global carbon (C) cycle, and excess N pollution has been identified as one of the three global environmental issues whose ‘planetary boundary’ has been surpassed¹. Once an N atom is in a reactive form (N_r), it cascades through different eco-system compartments, contributing to a number of environmental problems². Most of the anthropogenic N_r will be removed by denitrification, the reduction of oxidized forms of inorganic N to N₂O and, ultimately, inert N₂. However, estimates of terrestrial sinks for N_r are highly uncertain and the magnitude of total denitrification losses (N₂ + N₂O) is virtually unknown for the vast majority of agricultural soils. While there is increasing research investigating the soil-atmosphere exchange of N₂O in fertilized agro-ecosystems, information on N₂ emissions and related N₂:N₂O partitioning data is still scarce³. The main reasons for this uncertainty are that denitrification exhibits a very high spatial and temporal variability, but foremost that it is extremely difficult to measure N₂ emissions against the huge atmospheric N₂ background⁴.

Currently, there are only two main approaches for the direct quantification of denitrification N gas formation including N₂ and N₂O in the field: (1) the Acetylene Inhibition Technique (AIT) and (2) the ¹⁵N-gas flux method. The AIT is historically the most widely applied method to quantify denitrification in the field due to its relatively simple and inexpensive application. However, in recent years it has been shown that the AIT leads to a systematic and irreproducible underestimation of denitrification rates due a number of limitations^{3–6}, which preclude

¹Institute of Future Environments, Queensland University of Technology, Brisbane, QLD, 4000, Australia. ²Institute for Meteorology and Climate Research- Atmospheric Environmental Research (IMK-IFU), Karlsruhe Institute of Technology (KIT), Garmisch-Partenkirchen, Germany. Correspondence and requests for materials should be addressed to C.S. (email: clemens.scheer@kit.edu) or J.F. (email: johannes.friedl@qut.edu.au)

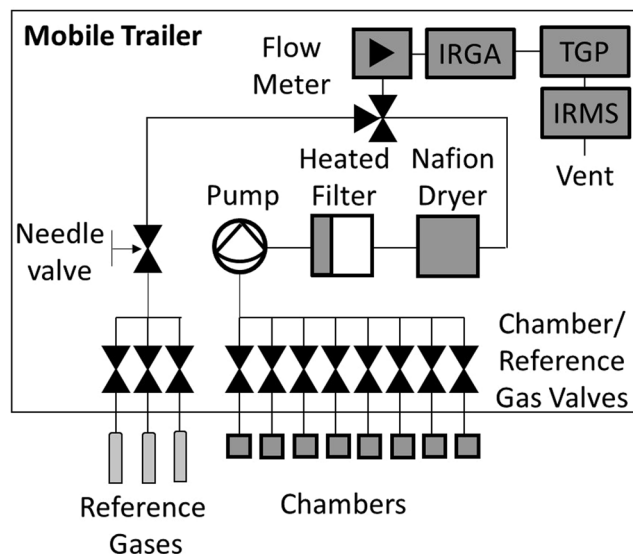


Figure 1. The setup of the field-based IRMS system: Automated chambers and the sampling and reference gas injection unit, the infra-red gas analyser (IRGA), the trace-gas preparation unit (TGP) and the IRMS.

reliable estimates of total denitrification losses⁷. The shortcomings of the AIT therefore demand the use of alternative methods when quantifying denitrification losses from agro-ecosystems. The ¹⁵N-gas flux method avoids the problems of the AIT, but requires expensive equipment as well as the costly application of highly ¹⁵N enriched fertilizer. ¹⁵N is added as highly enriched (20–80 atom %) fertilizer to a designated plot of soil which is then enclosed with a chamber prior to gas sampling. N₂ and N₂O gas production following denitrification is measured by quantifying the increase in ¹⁵N-labelled gases in the headspace using Isotope Ratio Mass Spectrometry (IRMS)⁸. The major challenges of the ¹⁵N tracing technique are (1) achieving and assessing uniform distribution of the isotopically labelled N in the soil (2) artificial stimulation of denitrification by the added tracer (3) high detection limits for N₂ fluxes due to analytical limitations in the *m/z* 30 measurements with the IRMS. The uniform distribution of ¹⁵N in the soil nitrate (NO₃⁻) pool is usually achieved by applying ¹⁵N enriched fertilizers with water, resulting in increased soil moisture. Under field conditions it is unlikely to achieve homogeneity of the added ¹⁵N tracer with the soil NO₃⁻ pool, but it has been shown that accurate estimates of gaseous N losses can be made without uniform distribution of ¹⁵N in the soil when large amounts of highly enriched N fertilizer are applied⁹. Consequently, the ¹⁵N gas flux method is most applicable for fertilized cropping systems where large amounts of enriched N fertilizer with water can be applied and high fluxes of N₂ and N₂O can be expected.

Another constraint for field measurements of denitrification is the high temporal (diurnal, daily and seasonal) variability of N gas emissions that compromise flux estimates if not carried out with an adequate frequency. For N₂O fluxes it has been shown that daily sampling is required to achieve annual N₂O fluxes within 10% of the best estimate, while weekly to monthly sampling in cropping systems with highly episodic emission events can result in an overestimation of 256% and 935%, respectively¹⁰. To address this problem more and more studies are using automated static chamber systems that can capture highly episodic emissions, and the characteristic diurnality in emissions, by multiple sampling events over any 24-hour period. Such “high-frequency” measurements of N₂O have significantly improved N₂O flux estimates. However, such instrumentation has not been available for both N₂ and N₂O measurements.

Here we present a novel, mobile isotope ratio mass spectrometer (Field-IRMS) coupled to a fully automated chamber system, measuring N₂ and N₂O fluxes in real time at a sub-daily resolution. The Field-IRMS is housed in an air-conditioned trailer and can be transported to the desired field location. We tested the performance of the Field-IRMS investigating the effect of two different fertilizer rates on the magnitude and N₂:N₂O partitioning of denitrification losses from a sugarcane field in subtropical Australia.

Methods

Field-based IRMS system. The new Field-IRMS was developed by the Queensland University of Technology (QUT) in collaboration with Sercon (Sercon, Crewe, UK) and is housed in an air-conditioned trailer which can be transported to the desired field location. The system uses a standard continuous flow IRMS coupled to a fully automated chamber system, measuring N₂ and N₂O fluxes in real time at a sub-daily resolution. The measuring principle is based on the ¹⁵N gas flux method and uses highly ¹⁵N enriched (20–80 atom % ¹⁵N) fertilizer added to the soil which is then enclosed with a chamber for a designated time period. N₂ and N₂O gas production from denitrification is measured by quantifying the increase in ¹⁵N-labelled gases in the chamber atmosphere using IRMS⁸.

The new Field-IRMS comprises three main parts: The automated chambers, the sampling unit, and a Sercon Continuous Flow 20–22 IRMS with a custom built trace gas preparation unit (TGP) (Fig. 1).

Automated chambers. The system utilises the static closed chamber technique (non-steady-state, non-through flow) to capture N_2 and N_2O fluxes from soils. It consists of eight automated acrylic static chambers (500 mm \times 500 mm \times 150 mm) that are fixed on stainless steel bases inserted permanently into the soil to a depth of 100 mm and sealed air-tight during sampling by two lids that open and close via pneumatic actuators. It was assumed that molecular diffusion created homogeneous gas concentrations in the chamber headspace at sampling and no fan to mix the air inside the chamber was installed. To limit the temperature increase in the chambers during the closure times the acrylic panels on the side of the chambers were tinted while the panels on the two lids of each chamber were covered with reflective foam insulation. Each chamber is connected to a sampling control system by a non-reactive Teflon coated sample line and two pneumatic air lines (for lid open and shut operation).

Sampling unit. The sampling system houses the sample pump, sample valves, reference gas valves, sample flow meter, an infra-red CO_2 analyser for the measurement of soil CO_2 fluxes (LI-840, LI-COR Biosciences, US), and a filtering system (Fig. 1). It is designed to extract sample gas from 8 chamber and three reference gas locations, which can be injected into the TGP at precise times during the sampling cycle. Each chamber and reference gas cylinder is connected to a single solenoid valve (Bürkert, Ingelfingen, Germany) arranged in arrays of eight and three, respectively. When either of the chamber valves are opened a diaphragm pump (JAVAC, Australia), provides constant air flow (200 mL min^{-1}) to the TGP from the chamber selected. For reference gas injection a three port valve is used to isolate the chamber valves from the reference gas valve stream. An adjustable flow meter (Key Instruments, Hatfield, USA) ensures constant flow from the sampled chamber headspace. A heated 0.1 micron coalescing filter and Nafion™ dryer filter system (Perma Pure, Lakewood, USA) removes particulate and water vapour from the gas sample.

Trace gas preparation unit. The custom built TGP works on the same principle as the standard Sercon Cryoprep trace gas module (Sercon, Crewe, UK), which isolates and purifies discreet amounts of trace gases to be transferred to the IRMS for isotopic analysis. The installation of two six-port Valco valves (VICI-Valco Instruments, Houston, USA) allows the incoming sample flow to fill a 200 mL N_2O sample loop and 50 μ L N_2 sample loop (Fig. 2a). Once the sample loops are filled the sample is injected into the helium carrier flow (20 mL min^{-1}) of the TGP, along two separate pathways: an $N_2 + N_2O$ path and an N_2O path.

$N_2 + N_2O$ path. Along the $N_2 + N_2O$ path, the sample is passed through a Nafion™ tube, a reduction oven and a GC column (Fig. 2b). The Nafion™ tubes remove any remaining water still present in the sample. The reduction oven of reduced copper heated to 600 °C removes O_2 from the sample. This is essential because any O_2 left in the sample will interfere with the isotopic analysis due to the production of NO and thus m/z 30 in the ion source of the IRMS. Moreover, the copper furnace reduces any NO or N_2O to N_2 , which will be subsequently detected as N_2 . Hence, it needs to be noted that the $N_2 + N_2O$ path will also contain any NO emitted from the soil which could result in an overestimation of the total N_2 fluxes. A molsieve (5 Å) packed GC column with a diameter of $\frac{1}{8}$ " and length of 20 cm separates N_2 from any remaining O_2 .

N_2O path. On the N_2O path, a Nafion™ tube, CO to CO_2 converter, CO_2 scrubber, and zeolite N_2O trapping system are installed. Once the N_2O sample is transferred to the helium carrier flow it first passes through the nafion tube to remove any residual water. The sample then passes through a two-part carbon scrubber: any CO in the sample is converted to CO_2 using a Schuetze reagent column, followed by a Carbosorb™ packed column removing CO_2 (Fig. 2c,d).

In commercially available trace gas preparation units, the isolation and concentration of N_2O is achieved using a liquid N (LN) trap. This requires a constant supply of LN which is not practical at remote field sites. The LN trap has therefore been replaced with a zeolite-based N_2O trapping system. The sample is passed through a cooled zeolite column for 423 seconds which effectively traps N_2O . Once the N_2O is trapped, the zeolite trap is isolated from the helium carrier stream by switching the respective Valco valve. The zeolite trap is then heated for 125 seconds, releasing the trapped N_2O . The now concentrated N_2O is then directed back into the helium carrier and transferred to the IRMS. To trap the N_2O , the zeolite is cooled to near 0 °C by using Peltier CPU coolers (RS Components, Sydney, Australia). Standard cartridge heaters (RS Components, Sydney, Australia) are used to rapidly heat the zeolite column to 150 °C and release the N_2O from the zeolite trap.

Automated sampling cycle. The N_2 and N_2O fluxes are measured using a fully automated sampling cycle during which four gas samples are taken sequentially from each chamber over a 201.67 min period with a total closure time of 221.83 min. During each of the sampling runs different reference standards are analysed alternating with the samples. The reference standards consisted of ambient air samples and a 1 ppm N_2O standard, injected from a certified calibration gas cylinder (SupaGas, Beenleigh, QLD, Australia). The ambient air samples were used to provide an isotopic reference for the N_2 measurements, and the N_2O calibration standard was used to provide a reference for the N_2O measurements. More details of the automated sampling cycle are provided in the Supporting Information.

Flux calculations. Di-nitrogen and the converted N_2O ($N_2 + N_2O$) are measured as N_2 in the IRMS, while N_2O is measured directly as N_2O . For N_2O , the ion currents (I) at m/z 44, 45 and 46 enabled the calculation of the molecular ratios ^{45}R ($^{45}I/^{44}I$) and ^{46}R ($^{46}I/^{44}I$), giving the fraction of N_2O derived from the NO_3^- pool undergoing denitrification of the enrichment aD^{11} . The concentration of N_2O is calculated based on measured (^{45}R , ^{46}R) and calculated (^{47}R , ^{48}R) ratios of N_2O isotopologues in each sample compared to those in of the 1 ppm reference¹². For N_2 , the I at m/z 28, 29 and 30 enabled ^{29}R ($^{29}I/^{28}I$) and ^{30}R ($^{30}I/^{28}I$) to be calculated, with differences between ambient and enriched atmospheres expressed as $\Delta^{29}R$ and $\Delta^{30}R$. The flux of $N_2 + N_2O$ was calculated using $\Delta^{30}R$

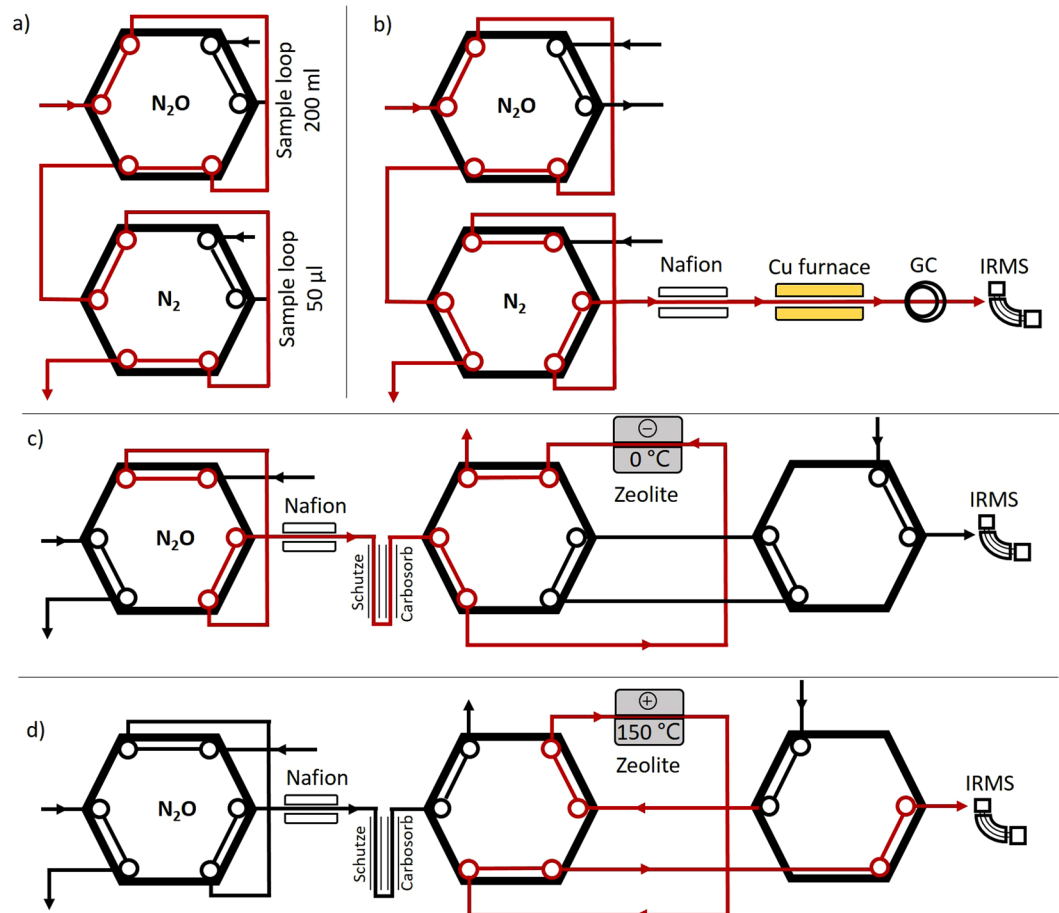


Figure 2. The trace gas preparation unit, with (a) N_2 and N_2O sample loop in filling position (b) the N_2 sample loop switched to the N_2 analysis path (c) the N_2O sample loop switched the N_2O path, trapping N_2O in the Zeolite trap, and (d) the release of N_2O to the IRMS, after the heating of the Zeolite trap.

and $\alpha D^{11,13}$, assuming that both N_2O and N_2 were produced from a single source pool. Flux rates of N_2O were calculated from the slope of the linear increase in gas concentration during the closure period. Fluxes of N_2 were then calculated as the difference between $N_2 + N_2O$ and N_2O fluxes. The coefficient of determination (r^2) was used for both $N_2 + N_2O$ and N_2O as a quality check for linearity and flux rates were discarded if r^2 was <0.80 (Fig. S1). Flux rates were corrected for temperature, air pressure and the ratio of cover volume to surface area¹⁴. For more details, see Supporting Information.

Field experiment. To test the performance of the novel system under field conditions we investigated the effect of two different fertilizer rates on the magnitude and the partitioning of N_2 and N_2O denitrification losses from a sugarcane cropping system in subtropical Australia (24°57'53"S, 152°20'0"E). Fertilizer ($K^{15}NO_3$ at 60 atom %, Sigma Aldrich) was applied to the chamber bases at a rate of 50 kg N ha⁻¹ (50 N) and 100 kg N ha⁻¹ (100 N), with four replicates arranged randomly along two sugarcane rows. The fertilizer was dissolved into 1 L of water and applied by hand, to each chamber, to ensure even distribution. Prior to the application of the fertilizer 3 L of water was applied to each chamber to ensure a wet soil profile while minimizing the potential for leaching losses of ^{15}N labelled fertilizer. Following the application of the fertilizer, a 5 cm thick layer of sugarcane trash was placed in each chamber and irrigated with a further 6 L of rainwater. Therefore, a total of 10 L irrigation was added to each chamber, which simulated a 50 mm rain event to completely saturate the soil. The addition of the sugarcane trash is consistent with farming practices in the growing region. More details of the experimental site are given in the Supporting Information.

Soil sampling and analysis. Initial soil samples were taken to 10 cm depth before fertilizer application and after four days from each edge and the centre of each soil frame using a 5 cm soil auger. One day after the final N_2 and N_2O flux measurements, final soil samples were taken from the profile in 10 cm increments to a depth of 50 cm.

The soil samples were analysed for total mineral N by extracting the NH_4^+ and NO_3^- in a 20 g subsample of soil. The subsamples were mixed in 100 mL of KCl (1:5 solutions) and shaken for one hr before being filtered through Whatman no. 42 filter paper. The KCl extracts were then analysed for N- NH_4^+ and N- NO_3^- on an AQ2+ discrete analyser (SEAL Analytical WI, USA).

Treatment	Total N lost	N ₂	N ₂ O	N ₂ O _d	Product ratio of denitrification
	kg N – N ₂ + N ₂ O ha ⁻¹	kg N – N ₂ ha ⁻¹	kg N – N ₂ O ha ⁻¹	kg N – N ₂ O _d ha ⁻¹	N ₂ /(N ₂ + N ₂ O _d)
50 N	2.10 ± 0.46 ^a	1.97 ± 0.44 ^a	0.13 ± 0.04 ^a	0.10 ± 0.03 ^a	0.93 ± 0.02 ^a
100 N	6.12 ± 0.99 ^b	5.45 ± 0.78 ^b	0.67 ± 0.22 ^a	0.61 ± 0.2 ^a	0.90 ± 0.02 ^a

Table 1. Total N losses and the resulting product ratio of denitrification (N₂/N₂ + N₂O ratio) over the seven day monitoring period. Means denoted by a different lowercase letter indicate significant differences ($P < 0.05$) between treatments.

The ¹⁵N enrichments of the N-NO₃⁻ and N-NH₄⁺ was determined for the 0–10 cm samples by the diffusion method¹⁵. After the diffusion process was complete, the samples were analysed on a Sercon 20–22 IRMS.

Auxiliary measurements. Soil moisture and temperate was measured at a depth of 10 cm in four of the eight chambers using automatic probes (HOBOnodes, Onset, USA). These probes collected moisture and temperature reading every 5 seconds for the duration of the experiment. Chamber temperature was also recorded in one chamber of each set.

Statistical analysis. Statistical analyses were conducted with SPSS 22.0 (SPSS Inc., 2013). Treatment effects on N₂ and N₂O fluxes were examined by analysis of variance (ANOVA) ($P < 0.05$). Changes over time were analysed using one way repeated measures ANOVA ($P < 0.05$), where time was the repeated factor. Values in the figures represent means ± standard error of the mean.

Results

Performance of the Field-IRMS system. The precision of the Field-IRMS for N₂ analysis was evaluated using the between – batch standard deviation of ambient air samples ($n = 126$) included in the sampling run over the seven-day experimental period. The detection limit (DL) of N₂ was calculated based on the standard deviation (SD) of these atmospheric air samples. The SD was 2.85×10^{-07} and 8.55×10^{-07} for the true mass ratios ²⁹R (29/28) and ³⁰R (30/28), respectively. The detection limit was calculated using equation 1:

$$DL = T_{(n-1, 1-\alpha=0.95)} * SD \quad (1)$$

where $T_{(n-1, 1-\alpha=0.95)}$ is the student's t value at a 95% confidence level at $n-1$ degrees of freedom and SD is the respective standard deviation. The between batch DL of the Field-IRMS at the 95% confidence interval ($n = 126$) for ²⁹R was 4.70×10^{-07} and for ³⁰R was 1.41×10^{-06} . This equates to a method DL (MDL) for N₂ fluxes of $54 \text{ g ha}^{-1} \text{ day}^{-1}$ of N₂ based on a NO₃⁻ ¹⁵N pool enrichment of 50% and a closure time of 201 minutes.

The precision of the IRMS for N₂O measurements was determined based on repeated analyses of an N₂O gas standard ($n = 12$) with a concentration of 1 ppm at natural abundance injected into the TPG unit. The SD was 3.79×10^{-04} and 9.08×10^{-05} for the true mass ratios ⁴⁵R (45/44) and ⁴⁶R (46/44), respectively. The SD of the N₂O concentration was 0.013 ppm, which equates to a DL at a 95% confidence interval of 0.02 ppm (equation 1). The resulting MDL for N₂O was $0.25 \text{ g N}_2\text{O-N ha}^{-1} \text{ day}^{-1}$.

Field test. We were able to measure significant fluxes of both N₂ and N₂O over the entire seven day field test in the sugarcane cropping system, with a significant accumulation of ¹⁵N-N₂ and N₂O in the chamber headspace over the 201 min measuring time (Fig. S1). For N₂O a linear increase in the chamber headspace could be confirmed, with $r^2 > 0.9$ for the regression of the N₂O concentration versus time for all measurements. For N₂ a linear increase in ¹⁵N-N₂ over time was confirmed for most measurements with $r^2 > 0.8$ for the regression of the ¹⁵N concentration versus time for 93% of all flux measurements, while 7% of the fluxes were discarded. The enrichment of the soil NO₃⁻ pool undergoing denitrification derived from ¹⁵N₂O (*aD*) and from ¹⁵N₂ were not significantly different, except for two days in each treatment (Fig. S2).

Total N₂ + N₂O losses over the seven-day monitoring period resulted in $2.10 \pm 0.46 \text{ kg ha}^{-1}$ and $6.12 \pm 0.99 \text{ kg ha}^{-1}$ lost for the 50 N and 100 N treatments, respectively (Table 1). N₂O from denitrification (N₂O_d) accounted for 78% (50 N) and 91% (100 N) of total N₂O emissions. N₂ was the main product of denitrification in both treatments, with an N₂/(N₂ + N₂O) product ratio of 0.93 and 0.90 of the total in the 50 N and 100 N treatment, respectively. Cumulative N₂ emissions exceeded N₂O emissions by a factor of 10 ± 2 in the 50 N treatment and a factor of 17 ± 5 in the 100 N treatment. Of the cumulative denitrification losses (N₂ + N₂O) 77% and 80% were fertilizer derived in the 50 N and 100 N treatments, respectively.

The temporal pattern of mean N₂ fluxes shows a pulse of N₂ emissions after fertilization and of irrigation (Fig. 3). On day one, $0.39 \pm 0.17 \text{ g N}_2\text{-N ha}^{-1} \text{ day}^{-1}$ and $0.98 \text{ kg} \pm 0.23 \text{ N}_2\text{-N ha}^{-1} \text{ day}^{-1}$ were emitted from the 50 N and 100 N treatment, respectively. Subsequent N₂ fluxes decreased in both treatments with lowest N₂ fluxes at day 3 regardless of treatment. A second irrigation event of 25 mm during the night of the 3rd day led to a second peak in N₂ emissions on day 5, with N₂ fluxes of $0.40 \pm 0.08 \text{ g N}_2\text{-N ha}^{-1} \text{ day}^{-1}$ and $1.25 \pm 0.28 \text{ kg N}_2\text{-N ha}^{-1} \text{ day}^{-1}$ for the 50 N and 100 N treatment, respectively.

Nitrous oxide emissions were highest on day 1 in both treatments and decreased over the course of the experiment (Fig. 3), exhibiting a small spike on day 4 in both treatments. Nitrous oxide from the 50 N treatment decreased from $65.4 \pm 28.70 \text{ g N}_2\text{O-N ha}^{-1} \text{ day}^{-1}$ on day 1 to $7.6 \pm 1.64 \text{ g N}_2\text{O-N ha}^{-1} \text{ day}^{-1}$ on day 7. In the

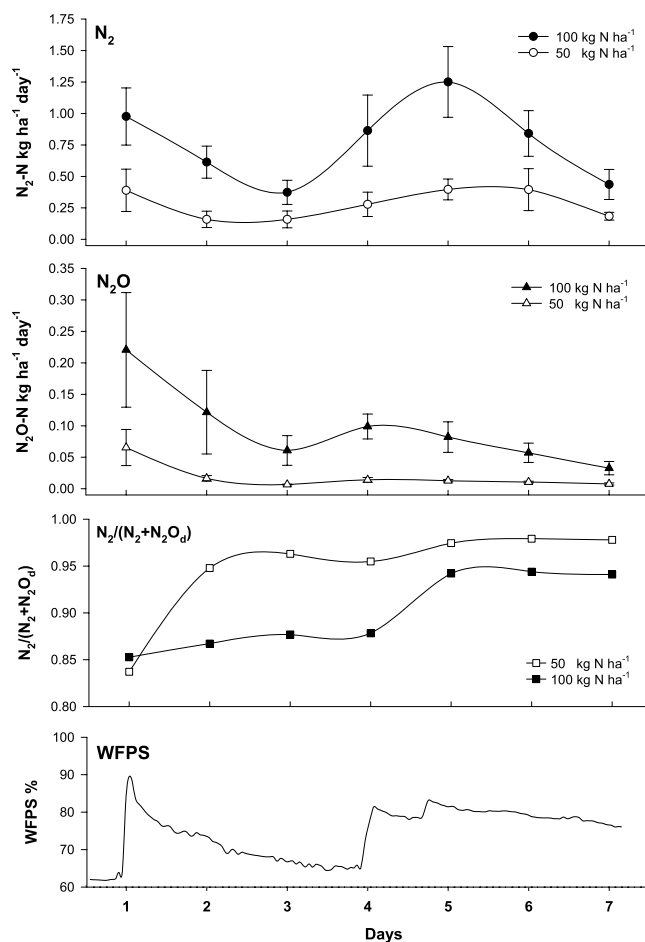


Figure 3. Temporal pattern of N_2 and N_2O fluxes ($kg\ N\ ha^{-1}\ day^{-1}$) and the corresponding product ratio of denitrification ($N_2/(N_2 + N_2O)$ ratio) over the seven day monitoring period for the two fertilizer application rates of 50 $kg\ N\ ha^{-1}$ and 100 $kg\ N\ ha^{-1}$. The bottom graph shows the water-filled pore space over the monitoring period based on hourly averages.

50 N treatment N_2O emissions peaked on day 1 at $221 \pm 9.11\ g\ N_2O-N\ ha^{-1}\ day^{-1}$ with a subsequent decrease to $32.7 \pm 1.06\ g\ N_2O-N\ ha^{-1}\ day^{-1}$ on day 7.

The temporal pattern of product ratio of denitrification ($N_2/(N_2 + N_2O)$) shows N_2 as the main product of denitrification over the entire course of the experiment in both treatments (Fig. 3). Lowest ratios were observed on day one at 0.84 and 0.85, for the 50 N and 100 N treatment, respectively. In the 50 N treatment, the $N_2/(N_2 + N_2O)$ increased above 0.90 after day 1 to 0.98 at day 7, while the $N_2/(N_2 + N_2O)$ ratio of the 100 N treatment remained below 0.90 until day 5, increasing to 0.94 at day 7.

The soil NO_3^- concentration decreased over the first 4 days of the experiment in both treatments to less than 20% of the initially applied fertilizer (Table 2). This rapid decline continued until day 8 with only 7% of the applied NO_3^- detectable in the top 10 cm of the soil. The enrichment of the $^{15}NO_3^-$ pool declined from a theoretical value of 55 atom% ^{15}N to values below 20 atom%. The soil NH_4^+ pool displayed no significant changes over time but exhibited ^{15}N enrichment over the course of the experiment indicating movement of the added $^{15}NO_3^-$ fertilizer into the soil NH_4^+ pool.

The ^{15}N enrichment of the NO_3^- pool undergoing denitrification (aD) was slightly lower than the theoretical ^{15}N enrichment calculated from the addition of labelled fertilizer at 60% atom $^{15}N-NO_3^-$ to the existing soil mineral N pool ($1.92\ kg\ NO_3^- N\ ha^{-1}$) at natural abundance (Table 2). There was no significant difference in aD between the two treatments and over time with average values of 0.48 and 0.46 for the 100 N and 50 N treatment, respectively.

Discussion

Performance of the novel Field-IRMS. The custom build Field-IRMS, a modified continuous flow IRMS coupled to a fully automated chamber system, enabled direct field measurements of N_2 and N_2O fluxes from ^{15}N labelled soil in real time at a sub-daily resolution. To our knowledge, this is the first time that automated real-time measurements of N_2 and N_2O from fertilized cropping systems are reported.

The most significant equipment modification was the sample preparation unit where we used a zeolite-based N_2O trapping system and included automated sampling loops to transfer the air samples from the field chambers into the helium carrier flow of the TGP. The new Field-IRMS allows for simultaneous analysis of concentration

Measurements	Treatment	Days		
		0	4	8
NO ₃ ⁻ (kg-N ha ⁻¹)	50 N	51.9*	9.13 ± 0.55 ^a	3.87 ± 1.51 ^b
	100 N	101.9*	18.44 ± 7.06 ^a	7.73 ± 4.61 ^{ab}
NH ₄ ⁺ (kg-N ha ⁻¹)	50 N	8.31	5.51 ± 0.43 ^a	6.04 ± 0.79 ^a
	100 N		5.84 ± 0.48 ^a	6.88 ± 0.47 ^a
¹⁵ NO ₃ ⁻ (atom% ¹⁵ N)	50 N	54.93*	28.77 ± 0.96 ^a	17.82 ± 3.26 ^a
	100 N	55.66*	29.10 ± 2.40 ^a	16.64 ± 7.47 ^a
¹⁵ NH ₄ ⁺ (atom% ¹⁵ N)	50 N	0.36	2.38 ± 0.76 ^a	1.84 ± 0.56 ^a
	100 N	0.36	2.71 ± 0.37 ^a	3.05 ± 0.36 ^a
<i>a</i> D	50 N	0.44 ± 0.01 ^a	0.45 ± 0.01 ^a	0.47 ± 0.01 ^a
	100 N	0.47 ± 0.04 ^a	0.48 ± 0.06 ^a	0.49 ± 0.07 ^a

Table 2. Soil mineral nitrogen levels (NO₃⁻-N, NH₄⁺-N), the ¹⁵N enrichment of the soil mineral nitrogen pools (NO₃⁻-¹⁵N, NH₄⁺-¹⁵N) and the fraction of the ¹⁵N labelled nitrate pool undergoing denitrification (*a*D)) at day 1, 4 and 8 of the field experiment. Means denoted by a different lowercase letter indicate significant differences (P < 0.05). *NO₃⁻ levels and enrichment for day 0 were calculated by mass balance from the amount and enrichment of the labelled fertilizer added to the soil.

and isotopic signature of N₂ and N₂O in the sample air with high analytical precision. The in batch standard deviation of atmospheric samples was used to define the instruments precision: For N₂, the standard deviation of ²⁹R was 4.70 * 10⁻⁰⁷, which is within the reported precision of other IRMS^{12,16}, while ³⁰R at 1.41 * 10⁻⁰⁶, was at the upper end of reported values¹⁷.

This precision of the IRMS translates to a detection limit of 53.9 g ha⁻¹ day⁻¹ and 0.25 g ha⁻¹ day⁻¹ for N₂ and N₂O emissions, respectively. These detection limits are comparable to or better than those reported by studies using the ¹⁵N gas flux method in fertilized cropping systems (62 to 380 g N ha⁻¹ day⁻¹ for N₂ and 1.0 to 1.7 g N ha⁻¹ day⁻¹ for N₂O)^{18–20}; but higher than those reported by a recent study that adapted the ¹⁵N gas flux method for application in unfertilized land use systems (1.0 g N ha⁻¹ day⁻¹ for N₂ and 0.05 * 10⁻³ g N ha⁻¹ day⁻¹ for N₂O)²¹. However, it needs to be noted that the MDL of the ¹⁵N gas flux method not only depends on the sensitivity of the IRMS and can potentially be lowered by (1) using a higher ¹⁵N enrichment of the applied fertilizer (2) decreasing the chamber volume and (3) increasing the closure time of the static chamber. All these parameters need to be adjusted according to the experimental set-up, in particular the expected N₂ and N₂O emission range.

To ensure high-quality measurements are provided, our automated chambers were designed using state of the art quality protocols^{22,23}. We chose to use relatively large chambers (basal area 0.25 m², height 0.15 m), to reduce the error associated with environmental variables such as temperature, the N₂O diffusion gradient within the soil and potential gas leaks into the chamber²⁴. Furthermore, the larger chambers account better for spatial variation, known to be one of the great challenges in measuring denitrification in the field²⁵, but require rather large amounts of costly ¹⁵N fertilizer.

Field studies using the ¹⁵N gas flux method in fertilized cropping systems typically only take two gas samples (t₀ and t₁) from the chamber over a 1 to 3 h closure time^{19,26,27}, but in unfertilized systems closure times up to 20 h have been reported^{21,28}. Long closure times have been shown to lead to an underestimation of denitrification rates due to decreasing concentration gradients between soil and chamber atmosphere, causing lowering of surface fluxes with increasing chamber deployment time and ideally, closure times should not exceed one hour²⁹. This means that for field measurements closure times should be minimised according to the expected N₂ and N₂O emission range but must be long enough so that sensitivity is not compromised. Our systems offers the advantage that four samples are taken over a closure period of 201 min which a) allows to check for the linearity of the evolved N₂ and N₂O gases over the deployment time of each individual chamber, b) increases the precision of the flux determination and c) enables a better quality control of the calculated flux including the detection of outliers.

Another key advantage of the Field-IRMS is that it eliminates any errors associated with the manual extraction, transport, storage and injection of gas samples and accounts for diurnal variations of the measured N gas fluxes. The limited amount of studies that reported N₂ fluxes from fertilized cropping systems typically used a sampling regime for N₂ measurements ranging from daily to weekly measurements, which cannot fully account for the high temporal variation of denitrification. Consequently, the use of an automated system will significantly improve estimates of denitrification from fertilized cropping systems. Such data is urgently needed for the identification of sustainable cropping practices that reduce GHG emissions and N pollution from agricultural systems while increasing food security under the auspices of climate change.

However, the accuracy of the ¹⁵N gas flux method needs to be revisited since recent research shows that field surface fluxes of ¹⁵N-labelled N₂ and N₂O emitted from ¹⁵N-labelled soil NO₃⁻ can severely underestimate denitrification due to subsoil flux and accumulation in pore space²⁹, suggesting that denitrification in fertilised cropping systems could even be more important than previously thought. Ideally, future studies on denitrification using the ¹⁵N-gas flux method can be combined with an estimation of subsoil fluxes.

Field experiment. Over the 7-day field campaign, significant N₂ and N₂O fluxes could be observed in both fertilizer treatments with 100% of the N₂O measurements and 93% of the N₂ measurements showing a significant linear increase in the chamber headspace, demonstrating the suitability of the new Field-IRMS to continuously measure N₂ and N₂O emissions in fertilized cropping systems. Denitrification was identified as a major loss

pathway of fertilizer N with total denitrification losses ($N_2 + N_2O$) of $2.10 \pm 0.46 \text{ kg ha}^{-1}$ and $6.12 \pm 0.99 \text{ kg ha}^{-1}$ over the seven-day period for the 50 N and 100 N treatments. These high N losses are in the range of previously reported values from sugarcane cropping systems in Australia^{27,30}. The only other study that used the ^{15}N gas flux method in a sugarcane field reported total denitrification losses ranging from 7.6 to 9.2 kg ha^{-1} over nine days after the application of 160 kg N ha^{-1} K^{15}NO_3 (98.5 atom %)²⁷. These results highlight that sub-tropical sugarcane systems in Australia can be a hotspot for soil denitrification where high denitrification losses can be expected in particular, since the high denitrification events occurred after 50 mm and 25 mm irrigation, respectively. Such rainfall events are characteristic for the humid subtropical summers in the study region and generally occur numerous times during the sugarcane growing season.

Fertilization and irrigation triggered an initial pulse of N_2 and N_2O emissions. High WFPS and NO_3^- availability together with soluble C from the sugarcane trash created conditions favouring denitrification, resulting in emissions of up to $1.25 \text{ kg N ha}^{-1} \text{ day}^{-1}$ of N_2 and N_2O combined. Following this first irrigation N_2 and N_2O emissions decreased over the first three days as the soil dried, while the $N_2:N_2O$ ratio shifted towards N_2 in the 50 N treatment. A second irrigation on the night of the third day resulted in a significant increase of N_2 while there was only a minor effect on N_2O emissions. Such a burst of N_2 and N_2O emissions following irrigation and fertilization has been observed in other cropping systems and is typically caused by O_2 depletion due to increased WFPS²⁶, and further amplified by increased N substrate availability and the formation of anaerobic microsites due to enhanced microbial activity and subsequent O_2 consumption^{31,32}. The increase in the $N_2/N_2 + N_2O$ product ratio over time reflects increasing anaerobic conditions in the soil matrix along with enhanced N_2O reductase activity, causing a shift towards complete denitrification to N_2 . The lower $N_2/(N_2 + N_2O)$ product ratio in the 100 N treatment can probably be attributed to higher soil NO_3^- concentrations³³ (Table 2), inhibiting N_2O reductase activity due to the competitive effect of NO_3^- and N_2O as electron acceptors during denitrification.

Total denitrification losses were 3 times higher in the 100 N treatment than in the 50 N treatment, while N_2O emissions were 5 times higher, which indicates that under the observed conditions of high moisture, temperature and C, denitrification was mainly limited by the NO_3^- availability and suggests a non-linear trend of increasing denitrification rates as N inputs increase to exceed crop needs, similar to what has been observed for N_2O emissions in fertilized cropping systems³⁴.

Denitrification was dominated by N_2 emissions, with an $N_2/(N_2 + N_2O)$ product ratio of 0.93 and 0.90 in the 50 N and 100 N treatment, respectively. These ratios are within the range of reported product ratios from other field studies that used the ^{15}N gas flux method in fertilized cropping systems^{19,26}, and agree well with the average product ratio of 0.85 ± 0.061 for fertilized agricultural soils by a recent meta-analysis that summarized available datasets where N_2 emissions have been either measured by ^{15}N -labelling approaches or with the gas-flow helium incubation method^{3,35}. However, it needs to be noted that the magnitude and the $N_2/(N_2 + N_2O)$ product ratio of denitrification is known to vary substantially depending on soil conditions and is primarily influenced by the soil nitrate content, the availability of easily degradable C substrates, soil moisture, soil oxygen content, the genetic potential for N_2O reduction and soil pH^{17,36–39}. Consequently, longer-term measurements from different sugarcane sites are ideally required to come up with robust estimates of $N_2/(N_2 + N_2O)$ product ratios and total denitrification losses for sugarcane cropping systems.

Another problematic aspect of the ^{15}N gas flux method is the determination of the ^{15}N enrichment of the source pool (NO_3^-). We used the isotopic signatures of $^{45}\text{N}_2\text{O}:$ $^{44}\text{N}_2\text{O}$ and $^{46}\text{N}_2\text{O}:$ $^{44}\text{N}_2\text{O}$ in the headspace gas to calculate the ^{15}N enrichment of the NO_3^- pool undergoing denitrification aD . While there was no statistically significant difference between the $^{15}\text{NO}_3^-$ pool undergoing denitrification derived from $^{15}\text{N}_2\text{O}$ (aD) and from $^{15}\text{N}_2$ (XN^{15}) (Fig. S2), XN^{15} was consistently lower than aD . This effect is in agreement with other studies and has been attributed to a non-homogeneity of tracer dilution as a result of small scale heterogeneity of nitrification resulting in a stronger dilution of the NO_3^- pool in oxic and lower dilution in anoxic microsites producing N_2 and N_2O ^{19,40}. But aD showed a much lower variation between replicates which suggests that the use of aD is under these conditions likely to be more reliable than XN^{15} , since d , the fraction of N_2O in the chamber headspace derived from denitrification is usually higher than the one for N_2 , as N_2O is a trace gas, supporting the use of aD to calculate N_2 fluxes¹¹.

On the first sampling day after application of ^{15}N fertilizer aD was 0.44 and 0.47 for the 50 N and 100 N treatment, respectively. This was lower than the theoretical value of 0.55 calculated by mass balance from the soil NO_3^- content before fertilizer application and the amount and enrichment of the labelled fertilizer added to soil, indicating increasing nitrification or heterogeneity in the initial NO_3^- distribution, and thus a higher contribution of non-fertilizer NO_3^- to the denitrifying NO_3^- pool. There was no significant change in aD over the course of the seven-day experiment, while measurements of the NO_3^- pool enrichment determined by the diffusion method following KCl extraction on day 4 and 8 of the experiment showed significantly lower values and a declining trend over time. The results of the diffusions show a dilution of the soil NO_3^- pools, most likely from nitrification of unlabelled NH_4^+ . However, this did not change the enrichment of the active denitrifying pool, which indicates a spatial separation of denitrification and nitrification, occurring in different micro-sites within the soil matrix. It has been shown that direct measurement of $^{15}\text{N}-\text{NO}_3^-$ using extraction and diffusion does not reflect the enrichment of the active NO_3^- pool undergoing denitrification, and the use of these data in denitrification rate calculations has been shown to result in unrealistically high N_2 flux rates^{20,41}.

The automated sampling cycle of the Field-IRMS provides robust estimates of $\Delta^{29}\text{R}$, $\Delta^{30}\text{R}$ and aD , allowing to (a) test key assumptions of the ^{15}N gas flux method and (b) to calculate N_2 fluxes based on 4 point measurements. This approach represents a significant improvement compared to two point measurements and increases the precision of the flux determination. There is however still room for improvement regarding the sensitivity of the IRMS and the time needed per sample. Further improvements of the TGP and the sampling cycle including the integration of reference gas pulses injected directly into the IRMS and an adaption of the closure time in high emitting agro-ecosystems could further increase the temporal resolution of the Field-IRMS. Another promising

approach could be to use this system with a reduced N₂ atmosphere in the chamber headspace. This method has recently been used in field and lab studies and shown that it can significantly reduce the detection limit for N₂ fluxes^{41,42}. However, it requires a rather complex set-up involving flushing of the headspace and the sub-soil with an artificial gas mixture that needs to be coupled to the automated sampling system. Improving and combining these novel approaches to measure N₂ could significantly improve our understanding of denitrification in fertilized and even natural agroecosystems.

References

1. Rockström, J. *et al.* Planetary boundaries: exploring the safe operating space for humanity (2009).
2. Galloway, J. N. *et al.* The nitrogen cascade. *AIBS Bulletin* **53**, 341–356 (2003).
3. Butterbach-Bahl, K., Baggs, E. M., Dannenmann, M., Kiese, R. & Zechmeister-Boltenstern, S. Nitrous oxide emissions from soils: how well do we understand the processes and their controls? *Philosophical Transactions of the Royal Society B: Biological Sciences* **368** (2013).
4. Groffman, P. M. *et al.* Methods for measuring denitrification: diverse approaches to a difficult problem. *Ecol. Appl.* **16**, 2091–2122 (2006).
5. Stevens, R. J. & Laughlin, R. J. Measurement of nitrous oxide and di-nitrogen emissions from agricultural soils. *Nutrient Cycling in Agroecosystems* **52**, 131–139, <https://doi.org/10.1023/A:1009715807023> (1998).
6. Bollmann, A. & Conrad, R. Enhancement by acetylene of the decomposition of nitric oxide in soil. *Soil Biology and Biochemistry* **29**, 1057–1066 (1997).
7. Felber, R., Conen, F., Flechard, C. R. & Neftel, A. Theoretical and practical limitations of the acetylene inhibition technique to determine total denitrification losses. *Biogeosciences* **9**, 4125–4138, <https://doi.org/10.5194/bg-9-4125-2012> (2012).
8. Mosier, A. R. & Schimel, D. S. (eds Knowles Roger *et al.*) 181–208 (Academic Press, 1993).
9. Mulvaney, R. L. & Vanden Heuvel, R. M. Evaluation of nitrogen-15 tracer techniques for direct measurement of denitrification in soil: IV. *Field Studies. Soil Sci. Soc. Am. J.* **52**, 1332–1337, <https://doi.org/10.2136/sssaj1988.03615995005200050023x> (1988).
10. Barton, L. *et al.* Sampling frequency affects estimates of annual nitrous oxide fluxes. *Scientific reports* **5** (2015).
11. Stevens, R. J. & Laughlin, R. J. Lowering the detection limit for dinitrogen using the enrichment of nitrous oxide. *Soil Biol. Biochem.* **33**, 1287–1289, [https://doi.org/10.1016/S0038-0717\(01\)00036-0](https://doi.org/10.1016/S0038-0717(01)00036-0) (2001).
12. Stevens, R. J., Laughlin, R. J., Atkins, G. J. & Prosser, S. J. Automated Determination of Nitrogen-15-Labeled Dinitrogen and Nitrous Oxide by Mass Spectrometry. *Soil Sci. Soc. Am. J.* **57**, 981–988, <https://doi.org/10.2136/sssaj1993.03615995005700040017x> (1993).
13. Mulvaney, R. Determination of ¹⁵N-Labeled Dinitrogen and Nitrous Oxide with Triple-Collector Mass Spectrometers I. *Soil Sci. Soc. Am. J.* **48**, 690–692 (1984).
14. Scheer, C. *et al.* Impact of nitrification inhibitor (DMPP) on soil nitrous oxide emissions from an intensive broccoli production system in sub-tropical Australia. *Soil Biol. Biochem.* **77**, 243–251, <https://doi.org/10.1016/j.soilbio.2014.07.006> (2014).
15. Stark, J. M. & Hart, S. C. Diffusion technique for preparing salt solutions, Kjeldahl digests, and persulfate digests for nitrogen-15 analysis. *Soil Sci. Soc. Am. J.* **60**, 1846–1855 (1996).
16. Lewicka-Szczebak, D., Well, R., Giesemann, A., Rohe, L. & Wolf, U. An enhanced technique for automated determination of ¹⁵N signatures of N₂, (N₂+N₂O) and N₂O in gas samples. *Rapid Communications in Mass Spectrometry* **27**, 1548–1558, <https://doi.org/10.1002/rcm.6605> (2013).
17. Friedl, J. *et al.* Denitrification losses from an intensively managed sub-tropical pasture – Impact of soil moisture on the partitioning of N₂ and N₂O emissions. *Soil Biology and Biochemistry* **92**, 58–66, <https://doi.org/10.1016/j.soilbio.2015.09.016> (2016).
18. Bergsma, T. T., Ostrom, N. E., Emmons, M. & Robertson, G. P. Measuring simultaneous fluxes from soil of N₂O and N₂ in the field using the ¹⁵N-gas “nonequilibrium” technique. *Environ. Sci. Technol.* **35**, 4307–4312 (2001).
19. Buchen, C. *et al.* Fluxes of N₂ and N₂O and contributing processes in summer after grassland renewal and grassland conversion to maize cropping on a Plaggic Anthrosol and a Histic Gleysol. *Soil Biol. Biochem.* **101**, 6–19 (2016).
20. Kulkarni, M. V., Burgin, A. J., Groffman, P. M. & Yavitt, J. B. Direct flux and ¹⁵N tracer methods for measuring denitrification in forest soils. *Biogeochemistry* **117**, 359–373 (2014).
21. Sgouridis, F., Stott, A. & Ullah, S. Application of the ¹⁵N gas-flux method for measuring *in situ* N₂ and N₂O fluxes due to denitrification in natural and semi-natural terrestrial ecosystems and comparison with the acetylene inhibition technique. *Biogeosciences* **13**, 1821–1835 (2016).
22. de Klein, C. & Harvey, M. *Nitrous Oxide Chamber Methodology Guidelines*. (Ministry for Primary Industries, 2013).
23. Parkin, T. B. & Venterea, R. T. USDA-ARS GRACEnet project protocols, chapter 3. Chamber-based trace gas flux measurements. *Sampling protocols. Beltsville, MD* p. 1–39 (2010).
24. Rochette, P. & Eriksen-Hamel, N. S. Chamber measurements of soil nitrous oxide flux: Are absolute values reliable? *Soil Sci. Soc. Am. J.* **72**, 331–342 (2008).
25. Groffman, P. M. *et al.* Challenges to incorporating spatially and temporally explicit phenomena (hotspots and hot moments) in denitrification models. *Biogeochemistry* **93**, 49–77, <https://doi.org/10.1007/s10533-008-9277-5> (2009).
26. Friedl, J., Scheer, C., Rowlings, D. W., Mumford, M. T. & Grace, P. R. The nitrification inhibitor DMPP (3,4-dimethylpyrazole phosphate) reduces N₂ emissions from intensively managed pastures in subtropical Australia. *Soil Biol. Biochem.* **108**, 55–64 (2017).
27. Weier, K., Rolston, D. & Thorburn, P. The potential for N losses via denitrification beneath a green cane trash blanket (1998).
28. Sgouridis, F. & Ullah, S. Relative Magnitude and Controls of *in Situ* N₂ and N₂O Fluxes due to Denitrification in Natural and Seminal Natural Terrestrial Ecosystems Using ¹⁵N Tracers. *Environmental Science & Technology* **49**, 14110–14119, <https://doi.org/10.1021/acs.est.5b03513> (2015).
29. Well, R., Maier, M., Lewicka-Szczebak, D., Köster, J. R. & Ruoss, N. Underestimation of denitrification rates from field application of the ¹⁵N gas flux method and its correction by gas diffusion modelling. *Biogeosciences Discuss.* **2018**, 1–22, <https://doi.org/10.5194/bg-2018-495> (2018).
30. Weier, K. L., McEwan, C. W., Vallis, I., Catchpole, V. R. & Myers, R. J. Potential for biological denitrification of fertilizer nitrogen in sugarcane soils. *Aust. J. Agric. Res.* **47**, 67–79 (1996).
31. Luo, J., Tillman, R. W. & Ball, P. R. Factors regulating denitrification in a soil under pasture. *Soil Biology and Biochemistry* **31**, 913–927, [https://doi.org/10.1016/S0038-0717\(99\)00013-9](https://doi.org/10.1016/S0038-0717(99)00013-9) (1999).
32. Azam, F., Müller, C., Weiske, A., Benckiser, G. & Ottow, J. Nitrification and denitrification as sources of atmospheric nitrous oxide – role of oxidizable carbon and applied nitrogen. *Biol. Fertility Soils* **35**, 54–61, <https://doi.org/10.1007/s00374-001-0441-5> (2002).
33. Senbayram, M., Chen, R., Budai, A., Bakken, L. & Dittert, K. N₂O emission and the N₂O/(N₂O+N₂) product ratio of denitrification as controlled by available carbon substrates and nitrate concentrations. *Agric., Ecosyst. Environ.* **147**, 4–12, <https://doi.org/10.1016/j.agee.2011.06.022> (2012).
34. Shcherbak, I., Millar, N. & Robertson, G. P. Global metaanalysis of the nonlinear response of soil nitrous oxide (N₂O) emissions to fertilizer nitrogen. *Proceedings of the National Academy of Sciences* **111**, 9199–9204 (2014).
35. Butterbach-Bahl, K., Baggs, E. M., Dannenmann, M., Kiese, R. & Zechmeister-Boltenstern, S. Appendix: Nitrous oxide emissions from soils: how well do we understand the processes and their controls? *Philosophical Transactions of the Royal Society B: Biological Sciences* **368** (2013).

36. Barton, L., McLay, C., Schipper, L. & Smith, C. Annual denitrification rates in agricultural and forest soils: a review. *Soil Res.* **37**, 1073–1094 (1999).
37. Dannenmann, M., Butterbach-Bahl, K., Gasche, R., Willibald, G. & Papen, H. Dinitrogen emissions and the N₂: N₂O emission ratio of a Rendzic Leptosol as influenced by pH and forest thinning. *Soil Biol. Biochem.* **40**, 2317–2323 (2008).
38. Dodla, S. K., Wang, J. J., DeLaune, R. D. & Cook, R. L. Denitrification potential and its relation to organic carbon quality in three coastal wetland soils. *Sci. Total Environ.* **407**, 471–480 (2008).
39. Weier, K. L., Doran, J. W., Power, J. F. & Walters, D. T. Denitrification and the dinitrogen/nitrous oxide ratio as affected by soil water, available carbon and nitrate. *Soil Sci. Soc. Am. J.* **57**, 66–72 (1993).
40. Deppe, M. *et al.* Soil N₂O fluxes and related processes in laboratory incubations simulating ammonium fertilizer depots. **104**, 68–80 (2017).
41. Scheer, C., Meier, R., Brüggemann, N., Grace, P. R. & Dannenmann, M. An improved ¹⁵N tracer approach to study denitrification and nitrogen turnover in soil incubations. *Rapid Commun. Mass Spectrom.* **30**, 2017–2026 (2016).
42. Well, R. *et al.* Improvement of the ¹⁵N gas flux method for *in situ* measurement of soil denitrification and its product stoichiometry. **33**, 437–448 (2019).

Acknowledgements

This research was undertaken as part of the National Agricultural Nitrous Oxide Research Program funded by the Australian Department of Agriculture. We thank Weijin Wang and the Queensland Government's Department of Agriculture and Fisheries for providing the study site and the farm staff during the field measuring campaign. We also thank Sam Barker and Sercon, UK for developing the custom built trace gas preparation unit.

Author Contributions

D.W., C.S., D.R., C.B. and P.G. designed the investigation. D.W. and C.S. conducted the field experiment. D.W., C.S. and J.F. interpreted the data. All authors were involved in writing the paper and approved the final manuscript.

Additional Information

Supplementary information accompanies this paper at <https://doi.org/10.1038/s41598-019-47451-7>.

Competing Interests: The authors declare no competing interests.

Publisher's note: Springer Nature remains neutral with regard to jurisdictional claims in published maps and institutional affiliations.



Open Access This article is licensed under a Creative Commons Attribution 4.0 International License, which permits use, sharing, adaptation, distribution and reproduction in any medium or format, as long as you give appropriate credit to the original author(s) and the source, provide a link to the Creative Commons license, and indicate if changes were made. The images or other third party material in this article are included in the article's Creative Commons license, unless indicated otherwise in a credit line to the material. If material is not included in the article's Creative Commons license and your intended use is not permitted by statutory regulation or exceeds the permitted use, you will need to obtain permission directly from the copyright holder. To view a copy of this license, visit <http://creativecommons.org/licenses/by/4.0/>.

© The Author(s) 2019